Available online at www.sciencedirect.com
ScienceDirect
International Journal of Impact Engineering 34 (2007) 1780–1796
INTERNATIONAL JOURNAL OF IMPACT ENGINEERING
www.elsevier.com/locate/ijimpeng

Damage model for anisotropic materials, and its application to analysis of stability and spallation

Z.G. Wei, R.C. Batra*

Department of Engineering Science and Mechanics, Virginia Polytechnic Institute and State University, M/C 0219, Blacksburg, VA 24061, USA

Received 14 February 2006; received in revised form 19 September 2006; accepted 4 October 2006
Available online 28 December 2006

Abstract

We use Bai's conservation equation for cracks, and Rice and Tracey's equation for the growth of a spherical void in an infinite medium to derive an evolution equation for damage in an anisotropic material. It is then used to delineate the instability strain in a thin anisotropic sheet deformed in a plane stress state of deformation, and obeying Hill's yield criterion. Assuming that strain- and strain-hardening, and thermal and damage softening of the material can be characterized by a relation similar to that proposed by Batra, the effect of various material parameters, and the anisotropy of the sheet on the instability strain has been quantified. It is found that only strain hardening and thermal softening exponents strongly influence the instability strain. The spallation strength, time to spallation, and the fragment size are also discussed.

Keywords: Sheet necking; Damage model; Void growth; Material anisotropy; Spallation

1. Introduction

Dynamic ductile fracture under a general state of stress is believed to be due to the nucleation, coalescence, and growth of voids; the widely used nucleation and growth (NAG) model has been reviewed by Curran et al. [1]. Many physically based damage models can be found in Voyiadjis et al. [2]. There is considerable interest in deriving damage evolution laws from microstructural considerations. Rice and Tracey [3] used a variational method to derive a growth law of a void in an infinite isotropic perfectly plastic matrix subjected to tractions at far away boundaries. Subsequently, Gurson [4] analyzed the growth of a void in quasistatic deformations of a representative volume element of an isotropic perfectly plastic material obeying von Mises yield criterion, and proposed a yield surface for a porous material whose radius decreases with an increase in porosity. Engineering materials usually have a large number of microvoids of various sizes. Thus a damage relation deduced from statistical mechanics is likely to be more relevant as has been done in [5–9] where microscopic mechanisms have been linked to macroscopic deformations of materials with voids, and a conservation

*Corresponding author. Tel.: +1 540 231 6051; fax: +1 540 231 4574.
E-mail address: rbatra@vt.edu (R.C. Batra).

0734-743X/$ - see front matter © 2006 Elsevier Ltd. All rights reserved.
doi:10.1016/j.ijimpeng.2006.10.002

equation has been derived. Wei and Batra [10] combined this conservation law with Rice and Tracey's [3] work to derive an evolution equation for damage in an isotropic material. However, many cold worked materials, such as sheet metals for stamping application usually are anisotropic. Liao et al. [11] analyzed plane stress deformations of a sheet containing a through-the-thickness hole, and used techniques similar to those employed by Gurson to propose a plastic potential for a body containing a single spherical void. This was adopted by Chien et al. [12] for studying, with the finite-element method, three-dimensional (3D) deformations of a cube containing a spherical void. In these analyses, the anisotropic matrix material was characterized by Hill's [13,14] yield criterion that is quadratic in stresses.

Here a statistical damage model of an anisotropic material is derived based on Bai et al.'s conservation law of microvoids, and the growth rate of a void in a finite anisotropic body. The growth rate of a single void is derived from the flow potential in anisotropic materials proposed by Liao et al. [11] with Hill's quadratic yield condition. The damage evolution law, and the modified Batra–Litonski thermo-viscoplastic constitutive relation is used to analyze the instability of sheet metals; factors affecting instability are numerically evaluated.

2. Development of a damage model

2.1. Incremental stress–strain relations

We assume that elastic deformations are negligible as compared to plastic deformations, the material can be modeled as rigid thermoviscoplastic, and the flow potential of the anisotropic material can be written as

$$f(\sigma_{ij},\sigma_{\mathrm{m}},\phi,\psi)=\overline{\sigma}^2+Y^2\left\{2\phi\,\cosh\left(\psi\frac{3\sigma_{\mathrm{m}}}{2Y}\right)-1-\phi^2\right\}=0, \tag{1}$$

where $\psi=\psi(F,\ G,\ H,\ L,\ M,\ N)$ is a function of the material anisotropy parameters, ϕ the porosity of a representative volume element, Y the yield stress, σ_{ij} the Cauchy stress tensor, σ_{m} the mean stress, and $\overline{\sigma}$ the equivalent stress defined below by Eq. (4). The associated flow rule is taken to be

$$\mathrm{d}\varepsilon_{ij}=\mathrm{d}\lambda\,\frac{\partial f}{\partial\sigma_{ij}}, \tag{2}$$

where $\mathrm{d}\lambda$ is the proportionality factor. The strain-rate tensor is defined by

$$\dot{\varepsilon}_{ij}=\frac{1}{2}\left(v_{i,j}+v_{j,i}\right),\quad i,j=1,2,3, \tag{3}$$

where v_i is the velocity, and a comma followed by index i designates partial derivative with respect to the rectangular Cartesian coordinate x_i. We set either $i=1,2,3$ or $i=x,y,z$.

The equivalent stress in an anisotropic material can be written as [13]

$$\overline{\sigma}=\sqrt{\frac{3}{2}}\left[\frac{F\left(\sigma_{yy}-\sigma_{zz}\right)^2+G(\sigma_{zz}-\sigma_{xx})^2+H\left(\sigma_{xx}-\sigma_{yy}\right)^2+2L\sigma_{yz}^2+2M\sigma_{xz}^2+2N\sigma_{xy}^2}{F+G+H}\right]^{1/2}. \tag{4}$$

Substitutions from Eq. (4) into Eq. (1), and the result into Eq. (2) give

$$\begin{aligned}
\mathrm{d}\varepsilon_{xx}&=\left\{\tfrac{3}{F+G+H}\left[H\left(\sigma_{xx}-\sigma_{yy}\right)+G(\sigma_{xx}-\sigma_{zz})\right]+\phi\psi Y\,\sinh\left(\psi\tfrac{3\sigma_{\mathrm{m}}}{2Y}\right)\right\}\mathrm{d}\lambda,\\
\mathrm{d}\varepsilon_{yy}&=\left\{\tfrac{3}{F+G+H}\left[F\left(\sigma_{yy}-\sigma_{zz}\right)+H\left(\sigma_{yy}-\sigma_{xx}\right)\right]+\phi\psi Y\,\sinh\left(\psi\tfrac{3\sigma_{\mathrm{m}}}{2Y}\right)\right\}\mathrm{d}\lambda,\\
\mathrm{d}\varepsilon_{zz}&=\left\{\tfrac{3}{F+G+H}\left[G(\sigma_{zz}-\sigma_{xx})+F\left(\sigma_{zz}-\sigma_{yy}\right)\right]+\phi\psi Y\,\sinh\left(\psi\tfrac{3\sigma_{\mathrm{m}}}{2Y}\right)\right\}\mathrm{d}\lambda,\\
\mathrm{d}\varepsilon_{xy}&=\mathrm{d}\varepsilon_{yx}=\tfrac{3}{F+G+H}N\sigma_{xy}\,\mathrm{d}\lambda,\\
\mathrm{d}\varepsilon_{xz}&=\mathrm{d}\varepsilon_{zx}=\tfrac{3}{F+G+H}M\sigma_{xz}\,\mathrm{d}\lambda,\\
\mathrm{d}\varepsilon_{yz}&=\mathrm{d}\varepsilon_{zy}=\tfrac{3}{F+G+H}L\sigma_{yz}\,\mathrm{d}\lambda,
\end{aligned} \tag{5}$$

where

$$\varepsilon_{ij} = \varepsilon_{ji}, \quad \sigma_{ij} = \sigma_{ji}.$$

The incremental volumetric strain can be expressed as

$$\mathrm{d}\varepsilon_v = \mathrm{d}\varepsilon_{ii} = 3\phi\psi Y \sinh\left(\psi \frac{3\sigma_{\mathrm{m}}}{2Y}\right) \mathrm{d}\lambda = \frac{\mathrm{d}\phi}{1-\phi}, \tag{6}$$

and the incremental deviatoric strain as

$$\mathrm{d}e_{ij} = \mathrm{d}\varepsilon_{ij} - \left(\mathrm{d}\varepsilon_v/3\right)\delta_{ij}. \tag{7}$$

We substitute in Eq. (7) for $\mathrm{d}\varepsilon_{ij}$ and $\mathrm{d}\varepsilon_v$ from Eqs. (5) and (6), and get

$$\begin{aligned}
\mathrm{d}e_{xx} &= \left\{\frac{3}{F+G+H}\left[H\left(\sigma_{xx}-\sigma_{yy}\right)+G(\sigma_{xx}-\sigma_{zz})\right]\right\}\mathrm{d}\lambda,\\
\mathrm{d}e_{yy} &= \left\{\frac{3}{F+G+H}\left[F\left(\sigma_{yy}-\sigma_{zz}\right)+H\left(\sigma_{yy}-\sigma_{xx}\right)\right]\right\}\mathrm{d}\lambda,\\
\mathrm{d}e_{zz} &= \left\{\frac{3}{F+G+H}\left[G(\sigma_{zz}-\sigma_{xx})+F\left(\sigma_{zz}-\sigma_{yy}\right)\right]\right\}\mathrm{d}\lambda,\\
\mathrm{d}e_{xy} &= \mathrm{d}e_{yx} = \mathrm{d}\varepsilon_{xy} = \frac{3}{F+G+H}N\sigma_{xy}\,\mathrm{d}\lambda,\\
\mathrm{d}e_{xz} &= \mathrm{d}e_{zx} = \mathrm{d}\varepsilon_{xz} = \frac{3}{F+G+H}M\sigma_{xz}\,\mathrm{d}\lambda,\\
\mathrm{d}e_{yz} &= \mathrm{d}e_{zy} = \mathrm{d}\varepsilon_{yz} = \frac{3}{F+G+H}L\sigma_{yz}\,\mathrm{d}\lambda.
\end{aligned} \tag{8}$$

The deviatoric stress tensor is defined by

$$s_{ij} = \sigma_{ij} - \sigma_m\delta_{ij} \tag{9}$$

and the mean stress σ_{m} by

$$\sigma_{\mathrm{m}} = \tfrac{1}{3}\sigma_{ii}. \tag{10}$$

The incremental equivalent strain, $\mathrm{d}\bar{\varepsilon}$, is the work-conjugate of the equivalent stress $\bar{\sigma}$, i.e.,

$$s_{ij}\,\mathrm{d}e_{ij} = \bar{\sigma}\,\mathrm{d}\bar{\varepsilon}. \tag{11}$$

Substitutions from Eqs. (8) and (9) into Eq. (11), and using the definition (4) of the equivalent stress, we have

$$\mathrm{d}\lambda = \frac{\mathrm{d}\bar{\varepsilon}}{2\bar{\sigma}} \tag{12}$$

and

$$\begin{aligned}
\mathrm{d}\bar{\varepsilon} = \sqrt{\frac{2}{3}}\Bigg[&\frac{F\left(G\,\mathrm{d}e_{yy}-H\,\mathrm{d}e_{zz}\right)^2+G(H\,\mathrm{d}e_{zz}-F\,\mathrm{d}e_{xx})^2+H\left(F\,\mathrm{d}e_{xx}-G\,\mathrm{d}e_{yy}\right)^2}{(FG+GH+FH)^2}\\
&+2\left(\frac{\mathrm{d}e_{xy}^2}{N}+\frac{\mathrm{d}e_{xz}^2}{M}+\frac{\mathrm{d}e_{yz}^2}{L}\right)\Bigg]^{1/2}.
\end{aligned} \tag{13}$$

Four special cases are listed below:

(a) For $\phi = 0$, Eq. (1) reduces to the familiar flow surface for a perfectly plastic non-porous anisotropic solid [14].
(b) For $\sigma_{\mathrm{m}} = 0$, Eq. (1) becomes

$$\bar{\sigma} = Y(1-\phi). \tag{14}$$

Thus the yield strength of the porous material under zero mean stress is degraded by the factor $(1-\phi)$.

(c) For zero equivalent stress ($\overline{\sigma}=0$), Eq. (1) becomes

$$\sigma_{\mathrm{m}}=\left(\frac{2Y}{3\psi}\right)\cosh^{-1}\left[\left(1+\phi^2\right)/2\phi\right] \tag{15}$$

which by using the identity

$$\cosh^{-1}\left[\left(1+\phi^2\right)/2\phi\right]=\pm\ln\,\phi \tag{16}$$

can be written as

$$\sigma_{\mathrm{m}}=\left(\frac{2Y}{3\psi}\right)\ln\left(\frac{1}{\phi}\right). \tag{17}$$

Thus the threshold mean stress for void growth in an anisotropic solid is the same as that for an isotropic solid; Eq. (17) for an isotropic solid was derived by Carroll and Holt [15]. For a general anisotropic material, the function ψ can be determined by employing techniques similar to those of Rice and Tracey [3], and of Gurson [4]. However, we do not pursue this here, and only consider a normal anisotropic material for which the function ψ, proposed by Liao et al. [11], is given by

$$\psi=\sqrt{\frac{2(2R+1)}{3(R+1)}}, \tag{18}$$

where R characterizes the anisotropy of a plastic material [14].

(d) For a non-porous isotropic material ($\phi=0$) deformed under a uniaxial state of stress applied along the x-axis,

$$\begin{aligned} &s_{xx}=\frac{2\sigma}{3},\quad s_{yy}=s_{zz}=-\frac{\sigma}{3},\\ &\mathrm{d}\varepsilon_{xx}=\mathrm{d}\overline{\varepsilon},\quad \mathrm{d}\varepsilon_{yy}=\mathrm{d}\varepsilon_{zz}=-\mathrm{d}\overline{\varepsilon}/2,\quad \mathrm{d}\varepsilon_{v}=0. \end{aligned} \tag{19}$$

Thus for a nonporous isotropic material subjected to a uniaxial stress state, $\mathrm{d}\overline{\varepsilon}$ is simply the component of the plastic strain in the direction of the uniaxial stress.

2.2. Growth rate of a void

In an anisotropic material, the rate of change of radius, r, of a spherical void is related to the volumetric strain rate in the material. Substituting from Eqs. (6) and (12) into $\dot{r}/r=\dot{\phi}/3\phi$, we get

$$\frac{\dot{r}}{r}=(1-\phi)\psi Y\,\sinh\left(\psi\frac{3\sigma_{\mathrm{m}}}{2Y}\right)\frac{\dot{\overline{\varepsilon}}}{2\overline{\sigma}}\simeq\frac{1}{2}\psi\,\sinh\left(\psi\frac{3\sigma_{\mathrm{m}}}{2Y}\right)\dot{\overline{\varepsilon}}\simeq\frac{1}{4}\psi\exp\left(\psi\frac{3\sigma_{\mathrm{m}}}{2Y}\right)\dot{\overline{\varepsilon}}, \tag{20}$$

where we have tacitly assumed that $\sigma_{\mathrm{m}}\geqslant 0$. The last two expressions in Eq. (20) are valid approximately for small values of σ_{m} since Eq. (14) has been used.

Rice and Tracey [3] used the Rayleigh–Ritz method to derive the following relation for isotropic materials:

$$\frac{\dot{r}}{r}=0.283\,\exp\left(\frac{3\sigma_{\mathrm{m}}}{2Y}\right)\dot{\overline{\varepsilon}}. \tag{21}$$

For an isotropic material, $\psi=1$ as mentioned by Johnson [16], and the right-hand sides of Eqs. (20) and (21) are nearly equal. By using a more accurate mathematical treatment Huang et al. [17,18] revisited Rice and Tracey's [3] analysis, derived the following expression (22) for $\dot{r}/r$, and found that Rice and Tracey's relation (21) significantly underestimates the dilatation rate of an isolated void subject to stress fields with moderate to high triaxiality

$$\frac{\dot{r}}{r}=0.427\exp\left(\frac{3\sigma_{\mathrm{m}}}{2Y}\right)\dot{\overline{\varepsilon}}\ \text{for}\ \sigma_{\mathrm{m}}/Y\geqslant 1,$$

$$\frac{\dot{r}}{r} = 0.427\left(\sigma_m/Y\right)^{1/4} \exp\left(\frac{3\sigma_m}{2Y}\right)\dot{\bar{\varepsilon}} \text{ for } 1/3 \le \sigma_m/Y \leqslant 1. \tag{22}$$

We note that the right-hand side of Eq. (22) is 1.7 times that of Eq. (20) and 1.5 times that of Eq. (21). We will use Eqs. (18) and (20) to study growth of microvoids in anisotropic materials.

2.3. Statistical damage model

Following Bai et al.'s work [6,7] on ideal microcracks, we assume that during an initial stage of damage development:

(1) microvoids are spherical and sparsely distributed, thus the interaction among them is negligible;
(2) no new voids nucleate but the volume of existing voids can change; and
(3) the growth of a void is governed by macroscopic deformations.

Since voids of all shapes occur in a material, our assumption of voids being spherical necessarily gives us an approximate expression for the damage.

Both NAG of voids contribute to damage evolution and hence fracture initiation. However, the failure of ductile materials due to high tensile stresses is generally dominated by the rapid growth of voids (e.g. see [19]). The mechanisms of nucleation of voids are not clearly understood. Voids usually nucleate due to the debonding of the matrix from the inclusions and/or cracking of hard inclusions. Also, a microscopic material heterogeneity, such as structural discontinuities at surfaces, lines or points can generate a stress concentration and induce void formation. Empirical relations simulating either stress- or strain-controlled nucleation of voids have often been employed [20]. On the other hand, the growth of existing voids has been well studied, and is also considered here. The present work can be generalized to incorporate void nucleation once the mechanism has been better understood and appropriate relations have been established.

For simple and regular micro-voids, a micro-void can be represented by its volume υ. We now introduce the number-density (concentration in physical and phase space) of micro-voids, $n = n(\upsilon,t)$, defined as follows. At time t, the number of micro-voids of volume between υ and $\upsilon + \mathrm{d}\upsilon$ equals $n(\upsilon,t)\,\mathrm{d}\upsilon$. Initially, the expansion/contraction of micro-voids should change the number density n, since the interaction among micro-voids and their coalescence can be ignored. Thus the volume of voids can be written as

$$V_\upsilon = \int_0^\infty n(\upsilon,t)\upsilon\,\mathrm{d}\upsilon. \tag{23}$$

We assume that the number density of voids of volume υ changes with time according to the relation [6,7]:

$$\frac{\partial n}{\partial t} + \frac{\partial(n\dot{\upsilon})}{\partial \upsilon} = 0, \tag{24}$$

where a superimposed dot indicates the material time derivative. This equation is analogous to the continuity equation for an incompressible body.

We define a damage variable, D_υ, by

$$D_\upsilon = \frac{V_\upsilon}{V} = \frac{V - V_m}{V}, \quad \dot{D}_\upsilon \geqslant 0, \tag{25}$$

where V_m and V are, respectively, the volume of the matrix and of the representative volume element. Taking the material time derivative of both sides of Eq. (25) with respect to time t, we get

$$\dot{D}_\upsilon = \frac{1}{V}\dot{V}_\upsilon - \frac{D_\upsilon}{V}\dot{V}. \tag{26}$$

Thus the rate of damage evolution is due to the rate of change of void volume per unit volume of the body and also due to the rate of change of volume of the body. Recall that

$$\dot{V} = \dot{V}_m + \dot{V}_\upsilon = \dot{V}_\upsilon \tag{27}$$

since the matrix material is nearly incompressible, i.e., $\dot{V}_m \approx 0$. Substitution of Eq. (27) into Eq. (26) gives

$$\dot{D}_v = \frac{\dot{V}_v}{V}(1 - D_v). \tag{28}$$

Taking the time derivative of both sides of Eq. (23), we obtain

$$\dot{V}_v = \frac{\partial}{\partial t}\int_0^\infty n(v,t)\, v\, dv = \int_0^\infty \dot{n}\, v\, dv = -\int_0^\infty \frac{\partial\left(n\dot{v}\right)}{\partial v}\, v\, dv = \int_0^\infty n\dot{v}\, dv, \tag{29}$$

where we have used Eq. (24) and

$$\int_0^\infty \frac{\partial(n\dot{v})}{\partial v}\, v\, dv = nv\dot{v}\,|_0^\infty - \int_0^\infty n\dot{v}\, dv = -\int_0^\infty n\dot{v}\, dv, \tag{30}$$

as there are no voids of zero volume and no voids of infinite volume. Thus from the growth law of a single void, we can use statistical methods to derive the evolution equation of damage.

Recalling that $v = (4/3)\pi r^3$ and substituting for $\dot{r}$ from Eq. (20) into Eq. (29),we get

$$\dot{v} = 3 \times \frac{1}{4}\psi \exp\left(\psi\frac{3\sigma_m}{2Y}\right)\dot{\bar{\varepsilon}}\, v = \frac{3}{4}\psi \exp\left(\psi\frac{3\sigma_m}{2Y}\right)\dot{\bar{\varepsilon}}\, v \tag{31}$$

which when combined with Eqs. (28), (29) and (23) gives

$$\dot{D}_v = \frac{1}{V}\dot{V}_v(1 - D_v) = \frac{3}{4}\psi\, \exp\left(\psi\frac{3\sigma_m}{2Y}\right)\dot{\bar{\varepsilon}}\frac{V_v}{V}(1 - D_v) = \frac{3}{4}\psi\, \exp\left(\psi\frac{3\sigma_m}{2Y}\right)\dot{\bar{\varepsilon}}\, D_v(1 - D_v). \tag{32}$$

Eq. (32) gives the growth rate of damage as a function of the mean stress that is taken to be non-negative, the yield stress, the equivalent plastic strain rate, the anisotropy parameter and the current state of damage. For $\sigma_m < 0$, we set $\dot{D}_v = 0$.

For a two-dimensional (2D) problem the damage variable, D_s, is defined as the surface area of voids divided by the total area of cross section. For a spherical void of surface area s,

$$\frac{\dot{s}}{s} = \frac{2}{3}\frac{\dot{v}}{v}. \tag{33}$$

Thus substituting for $\dot{v}/v$ from Eq. (31) into Eq. (33) we get

$$\dot{D}_s = \frac{1}{2}\psi \exp\left(\psi\frac{3\sigma_m}{2Y}\right)\dot{\bar{\varepsilon}}\, D_s(1 - D_s). \tag{34}$$

Henceforth we omit the subscript s for brevity. When ψ and σ_m/Y are independent of $\bar{\varepsilon}$, we can integrate Eq. (34), and use the initial condition $D(t)|_{t=0} = D_0$ to obtain

$$D = \frac{D_0 \exp(K\bar{\varepsilon})}{[(1 - D_0) + D_0 \exp(K\bar{\varepsilon})]}$$
$$K = \frac{1}{2}\psi \exp\left(\psi\frac{3\sigma_m}{2Y}\right) \tag{35}$$

and

$$\frac{dD}{d\bar{\varepsilon}} = \frac{D_0(1 - D_0)\exp(K\bar{\varepsilon})}{[(1 - D_0) + D_0 \exp(K\bar{\varepsilon})]^2}. \tag{36}$$

For macroscopic isochoric deformations, the term $(1-D)$ in Eq. (34) equals one, and we get

$$D = D_0\, \exp(K\bar{\varepsilon}),$$
$$\frac{dD}{d\bar{\varepsilon}} = D_0 K\, \exp(K\bar{\varepsilon}) \tag{37}$$

which was also derived in [10]. Here we use Eqs. (35) and (36).

We note that by using Bai et al.'s statistical theory and void growth solution, Zhang et al. [21] have derived a damage evolution equation similar to Eq. (34). However, coefficients in the two equations differ because of different void growth models used. Zhang et al. [21] also compared predictions from four available growth models, and found that the void growth relations have the same form for the NAG [1,22], the Rice and Tracey [3], the Gurson [4], and the Johnson models [17], i.e., $\dot{r} \propto r$. We recently learned that the idea of combining Bai et al.'s statistical method with the void growth mechanism had been used by Feng et al. [23] though their formula differs from Eq. (34) since they employed a different growth mechanism. Feng et al. [23] derived the growth rate of a void from the balance between the surface energy a void creates and the plastic work dissipated during void's expansion. Li and Huang [24] studied a similar problem by using Bai's statistical theory, and the NAG model given in [22] for high stress triaxiality cases.

3. Instability of a thin sheet loaded in biaxial tension

Most sheet metal forming processes involve predominantly tensile strains; thus the maximum achievable deformation is limited by tensile instability such as necking. In a wide thin sheet, the deformation is initially uniform, and a plane stress state of deformation prevails. Considère [25] postulated that a structure becomes unstable at the maximum load, and derived an analytical expression for predicting diffuse necking. Swift [26] used the same criterion to derive conditions for diffuse necking in an isotropic sheet deformed in a plane stress state of deformation, and Mellor [27] derived the instability strain for different ratios of principal stresses. Swift's approach has been extended to anisotropic materials by Moore and Wallace [28] using Hills' yield criterion [14]; here we generalize Moore and Wallace's work by incorporating the effect of damage evolved during the deformation process.

Sheet instability and specifically the onset of sheet necking have also been studied by using Hill's criterion [29] for localized necking along a direction of zero extension. However, sheets stretched in biaxial tension have generally no direction of zero extension. Hecker [30] showed that the onset of necking can be represented by forming limit diagrams (FLDs) developed by Keeler [31]. A FLD is a 2D plot of the maximum and the minimum principal strains at which necking occurs in a sheet loaded in biaxial tension. Marciniak and Kuczynski [32] introduced a thickness imperfection, representing effective material inhomogenity rather than a physical reduction in the thickness, perpendicular to the principal stress direction and derived a condition for the onset of localized necking. There is an extensive literature on FLDs and several references can be found in [33].

Here we do not introduce any imperfection in the sheet, adopt Swift's [26] criterion, and postulate that an instability ensues in a biaxially loaded sheet when loads in the x_1- and the x_2-directions approach their extreme (maximum) values simultaneously and that the biaxial tension is applied through tensile tractions that are unaffected by local strain increments.

For simplicity, we orient our coordinate axes along the principal stress directions, and adopt the convention $1 = x$, $2 = y$, $3 = z$ with the z-axis aligned along the thickness direction. For a plane stress state, the effective stress can be written as

$$\overline{\sigma} = \overline{\sigma}(\sigma_1, \sigma_2), \tag{38}$$

where σ_1 and σ_2 are principal stresses, and Eq. (4) reduces to

$$\overline{\sigma} = \sqrt{\frac{3}{2}}\left[\frac{(G+H)\sigma_1^2 - 2H\sigma_1\sigma_2 + (F+H)\sigma_2^2}{F+G+H}\right]^{1/2}. \tag{39}$$

Since plastic deformations are assumed to be isochoric, $de_1 + de_2 + de_3 = 0$, and Eq. (13) can be approximated by

$$d\bar{\varepsilon} = \sqrt{\frac{2}{3}\frac{F+G+H}{FG+FH+GH}}\left[(F+H)\,de_1^2 + 2H\,de_1\,de_2 + (G+H)\,de_2^2\right]^{1/2}. \tag{40}$$

Here de_1 and de_2 are incremental strains along the directions of principal stresses σ_1 and σ_2. The onset of instability is characterized by

$$\begin{aligned} dF_1 &= \frac{d\sigma_1}{\sigma_1} + \frac{dA_1}{A_1} = 0, \\ dF_2 &= \frac{d\sigma_2}{\sigma_2} + \frac{dA_2}{A_2} = 0. \end{aligned} \tag{41}$$

With the definitions

$$-\frac{dA_1}{A_1} = d\varepsilon_1, \quad -\frac{dA_2}{A_2} = d\varepsilon_2, \tag{42}$$

we have

$$\begin{aligned} d\sigma_1 &= \sigma_1 d\varepsilon_1, \\ d\sigma_2 &= \sigma_2 d\varepsilon_2. \end{aligned} \tag{43}$$

We set

$$\alpha = \frac{\sigma_2}{\sigma_1}, \quad \gamma = \frac{d\varepsilon_2}{d\varepsilon_1} = \frac{de_2}{de_1}, \tag{44}$$

where we have neglected the change in volume due to the damage evolved. Thus

$$d\bar{\sigma} = \left[\frac{\partial\bar{\sigma}}{\partial\sigma_1} + \alpha\gamma\frac{\partial\bar{\sigma}}{\partial\sigma_2}\right]\sigma_1\, d\varepsilon_1 \tag{45}$$

which when combined with Eqs. (39) and (40) gives

$$\frac{d\bar{\sigma}}{d\bar{\varepsilon}} = \frac{\bar{\sigma}}{Z} \tag{46}$$

with

$$\begin{aligned} Z &= \sqrt{\frac{2}{3}}\frac{(F+G+H)^{1/2}\left[(G+H) - 2H\alpha + (F+H)\alpha^2\right]^{3/2}}{(F+H)^2\alpha^3 - H(2F+H)\alpha^2 - H(2G+H)\alpha + (G+H)^2} \\ &= \sqrt{\frac{2}{3}}\frac{(F+G+H)^{1/2}}{(FG+FH+GH)^{1/2}}\frac{\left[(F+H) + 2H\gamma + (G+H)\gamma^2\right]^{3/2}}{(F+H) + H\gamma + H\gamma^2 + (G+H)\gamma^3}, \end{aligned} \tag{47}$$

$$\alpha = \frac{(G+H)\gamma + H}{F+H+H\gamma}, \quad \gamma = \frac{(F+H)\alpha - H}{(G+H) - H\alpha}.$$

The instability criterion (46) is similar to that of Moore and Wallace [28], and does not explicitly depend upon the damage variable. This is due to definitions of incremental strains and the assumption (44) of the proportional stress and the proportional strain increments.

For a normal anisotropic material

$$\begin{aligned} Z &= \sqrt{\frac{2}{3}}\frac{(R+2)^{1/2}\left[(R+1) - 2R\alpha + (R+1)\alpha^2\right]^{3/2}}{(R+1)^2\alpha^3 - R(R+2)\alpha^2 - R(R+2)\alpha + (R+1)^2} \\ &= \sqrt{\frac{2}{3}}\frac{(R+2)^{1/2}}{(2R+1)^{1/2}}\frac{\left[(F+H) + 2H\gamma + (G+H)\gamma^2\right]^{3/2}}{(R+1) + R\gamma + R\gamma^2 + (R+1)\gamma^3} \end{aligned} \tag{48}$$

with

$$\alpha = \frac{(R+1)\gamma + R}{1+R+R\gamma}, \quad \gamma = \frac{(R+1)\alpha - R}{(R+1) - R\alpha}.$$

For an isotropic material, $R = 1$, and Eq. (48) simplifies to

$$Z = \frac{4\left(1-\alpha+\alpha^2\right)^{3/2}}{(1-\alpha)(4-7\alpha+4\alpha^2)} = \frac{4\left(1+\gamma+\gamma^2\right)^{3/2}}{\sqrt{3}(1+\gamma)(2-\gamma+2\gamma^2)}, \tag{49}$$

$$\alpha = \frac{2\gamma+1}{2+\gamma}, \quad \gamma = \frac{2\alpha-1}{2-\alpha}.$$

which are the same as those derived by Swift [26]. For uniaxial loading, $\alpha = 0$, $Z = 1$, and Considère's criterion is recovered.

3.1. Modified Batra–Litonski's thermo-viscoplastic constitutive relation

Batra [34] generalized Litonski's relation [35] for simple shearing deformations to that given below by Eq. (50) in which σ, ε and $\dot{\varepsilon}$ are the equivalent stress, the equivalent strain, and the equivalent strain rate, respectively, θ denotes the present temperature of a material particle, θ_0 its temperature in the undeformed reference configuration, and $\hat{\alpha}$, ε_y, b, n and m are material parameters; superimposed bars on σ, ε and $\dot{\varepsilon}$ have been omitted for simplicity

$$\sigma = \sigma_0\left(1+\frac{\varepsilon}{\varepsilon_y}\right)^n\left(1+b\dot{\varepsilon}\right)^m[1-\hat{\alpha}(\theta-\theta_0)]. \tag{50}$$

The flow stress σ in Eq. (50) should not be confused with the yield stres Y of the ideal rigid-plastic material appearing in Eq. (1). Wei and Batra [10] also considered the effect of material damage, and modified Eq. (50) to

$$\sigma = \sigma_0\left(1+\frac{\varepsilon}{\varepsilon_y}\right)^n\left(1+b\dot{\varepsilon}\right)^m\left(\frac{\theta_m-\theta}{\theta_m-\theta_r}\right)^v(1-D)^q, \tag{51}$$

where q is a material parameter. Note that terms specifying the dependence of the flow stress upon the temperature rise are different in Eqs. (50) and (51). In Eq. (51) thermal softening of the material is characterized by the exponent v, and the constant θ_m is usually referred to as the melting temperature of the material. However, it is a curve-fitting parameter and does not, in general, equal the melting temperature. θ_r in Eq. (51) equals the room temperature. When $D = 0$, there is no damage evolved, and when $D = 1$ the material has failed completely. The exponent q characterizes the dependence of the flow stress upon damage.

During a relatively high strain rate loading process, for example, when $\dot{\varepsilon} > 1/s$, heat conduction can be ignored if deformations have not localized into a narrow region generally called an adiabatic shear band. Batra and Kim [36] and Batra and Lear [37] have shown, through numerical experiments, that the time of initiation of an adiabatic shear band is virtually unaffected by neglecting effects of heat conduction. However, heat conduction affects significantly the post-localization response of the material. For locally adiabatic deformation, the temperature rise can be calculated from

$$\frac{d\theta}{d\varepsilon} = \frac{\beta\sigma}{\rho c}, \tag{52}$$

where $0 < \beta < 1$ is the Taylor–Quinney factor. Usually, $0.85 < \beta < 0.95$ for metals.

For deformations at a constant strain rate, the constitutive relation (50) can be substituted into Eq. (52), and the resulting equation can be integrated to arrive at Eq. (53). Eq. (54) gives the derivative of temperature with respect to the effective plastic strain. In the absence of damage, Eqs. (53) and (54) will give approximate values of the temperature rise, and its derivative with respect to the effective plastic strain

$$\theta = \theta_m - (\theta_m-\theta_r)\exp\left\{-\frac{\beta\sigma_0\varepsilon_y\left(1+b\dot{\varepsilon}\right)^m}{\rho c(\theta_m-\theta_r)(n+1)}\left[\left(1+\frac{\varepsilon}{\varepsilon_y}\right)^{n+1}-1\right]\right\} \text{ for } v = 1, \tag{53a}$$

$$\theta=\theta_{\mathrm{m}}-\left\{(\theta_{\mathrm{m}}-\theta_{\mathrm{r}})^{1-v}-\frac{\beta(1-v)\sigma_0\varepsilon_{\mathrm{y}}\left(1+b\dot{\bar{\varepsilon}}\right)^{m}}{\rho c(\theta_{\mathrm{m}}-\theta_{\mathrm{r}})^{v}(n+1)}\left[\left(1+\frac{\varepsilon}{\varepsilon_{\mathrm{y}}}\right)^{n+1}-1\right]\right\}^{1/(1-v)} \quad \text{for } v\neq 1, \tag{53b}$$

$$\frac{\mathrm{d}\theta}{\mathrm{d}\varepsilon}=\frac{\beta\sigma_0\left(1+b\dot{\bar{\varepsilon}}\right)^{m}}{\rho c}\left(1+\frac{\varepsilon}{\varepsilon_{\mathrm{y}}}\right)^{n}\exp\left\{-\frac{\beta\sigma_0\varepsilon_{\mathrm{y}}\left(1+b\dot{\bar{\varepsilon}}\right)^{m}}{\rho c(\theta_{\mathrm{m}}-\theta_{\mathrm{r}})(n+1)}\left[\left(1+\frac{\varepsilon}{\varepsilon_{\mathrm{y}}}\right)^{n+1}-1\right]\right\} \text{ for } v=1, \tag{54a}$$

$$\frac{\mathrm{d}\theta}{\mathrm{d}\varepsilon}=\frac{\beta\sigma_0\left(1+b\dot{\bar{\varepsilon}}\right)^{m}}{\rho c(\theta_{\mathrm{m}}-\theta_{\mathrm{r}})^{v}}\left(1+\frac{\varepsilon}{\varepsilon_{\mathrm{y}}}\right)^{n}\left\{(\theta_{\mathrm{m}}-\theta_{\mathrm{r}})^{1-v}-\frac{\beta(1-v)\sigma_0\varepsilon_{\mathrm{y}}\left(1+b\dot{\bar{\varepsilon}}\right)^{m}}{\rho c(\theta_{\mathrm{m}}-\theta_{\mathrm{r}})^{v}(n+1)}\left[\left(1+\frac{\varepsilon}{\varepsilon_{\mathrm{y}}}\right)^{n+1}-1\right]\right\}^{v/(1-v)} \quad \text{for } v\neq 1. \tag{54b}$$

For deformations at a constant strain-rate

$$\frac{\mathrm{d}\sigma}{\mathrm{d}\varepsilon}=\frac{\partial\sigma}{\partial\varepsilon}+\frac{\partial\sigma}{\partial\theta}\frac{\mathrm{d}\theta}{\mathrm{d}\varepsilon}+\frac{\partial\sigma}{\partial D}\frac{\mathrm{d}D}{\mathrm{d}\varepsilon}. \tag{55}$$

Substituting from Eq. (51) into Eqs. (55) and (46), we get the following instability criterion:

$$\frac{n}{\varepsilon_{\mathrm{y}}+\varepsilon}-\frac{v}{\theta_{\mathrm{m}}-\theta}\frac{\mathrm{d}\theta}{\mathrm{d}\varepsilon}-\frac{q}{1-D}\frac{\mathrm{d}D}{\mathrm{d}\varepsilon}=\frac{1}{Z}. \tag{56}$$

The derivatives of damage and temperature with respect to the effective plastic strain are given by Eqs. (36) and (54), respectively. Since the only unknown in Eq. (56) is the instability strain, the influence of material parameters upon it can be ascertained.

3.2. Results and discussion

We assume that the sheet is made of HY-100 steel, and list in Table 1 values of material parameters taken from [38]. Additionally, unless stated otherwise, we set $R=1.0$, $D_0=10^{-5}$, and $\sigma_2/\sigma_1=1$. For constant strain rate and proportional loading conditions, we delineate the effect of material parameters upon the instability strain by varying only one parameter at a time and keeping values of other parameters unchanged.

For different values of $\sigma_2/\sigma_1\leqslant 1$, Fig. 1 depicts the damage evolution with the axial strain computed from Eq. (35). After a slow start, the damage grows nearly exponentially, and at a given value of the axial strain, the damage evolved increases with an increase in σ_2/σ_1. For example, when $\sigma_2/\sigma_1=1$, the accumulated damage equals 0.3 at an axial strain of 7.7. We note that a material usually fails when the damage is about 0.3. However, the axial strain of 7.7 is much higher than that encountered in practice for most metals. Reasons for this discrepancy include the neglect in the mathematical model of several factors such as the generation of new voids, interaction among existing voids, coalescence of microvoids into a microcrack, and possibly inappropriate values of some material parameters. As shown below, the damage evolved plays a minor role when the axial strain in the x-direction is below the critical instability strain of about 0.1.

Fig. 2 exhibits, for different values of the anisotropy parameter R, the dependence upon the stress ratio σ_2/σ_1 of the instability strain in the x-direction. For each value of R considered, the instability strain ε_{I} first decreases, reaches a minimum value and subsequently increases. The value of σ_2/σ_1 at which ε_{I} attains a minimum value increases with an increase in the value of R.

Table 1
Values of material properties for the HY-100 steel

σ_0	n	m	v	ρ	c	ε_{y}	β	$\dot{\varepsilon}$	θ_{m}	θ_{r}	b	q
702 MPa	0.107	0.0117	1	7860 kg m^{-3}	473 J kg^{-1} K^{-1}	0.007	0.9	10/s	1500 K	300 K	17320/s	1

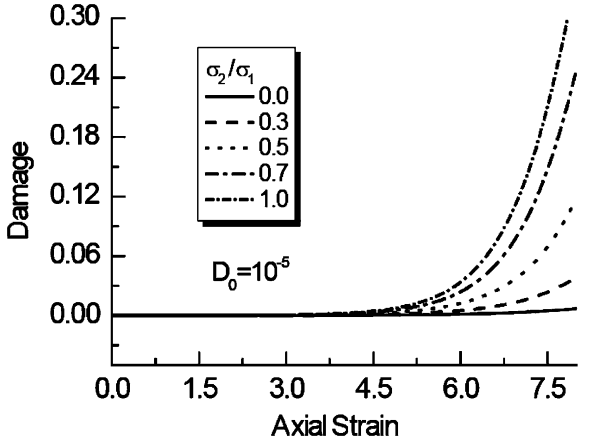

Fig. 1. For different values of σ_2/σ_1, damage evolution with the axial strain.

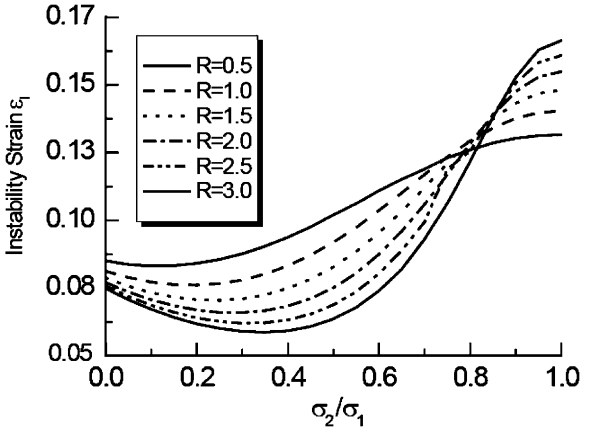

Fig. 2. For different values of the anisotropy parameter R, dependence of the instability strain upon σ_2/σ_1.

Results plotted in Fig. 2 also show that initially the instability strain decreases with an increase in the triaxiality ratio. For $R=1$ and small values of σ_2/σ_1 (e.g., $\sigma_2/\sigma_1<0.2$), $a=\varepsilon_{\text{minor}}/\varepsilon_{\text{major}}<0$ and ε_{I} is a decreasing function of σ_2/σ_1 which is consistent with that predicted by the Müschenborn and Sonne criterion [39] $\varepsilon_{\text{I}}=\varepsilon_{\text{major}}(4(1+a+a^2)/3)^{1/2}$ of necking in a sheet. Here $\varepsilon_{\text{minor}}$ and $\varepsilon_{\text{major}}$ are, respectively, the minor and the major strains (or the minimum and the maximum principal strains, respectively) at a point. However, for large values of σ_2/σ_1, $a>0$, and the instability strain increases with an increase in σ_2/σ_1 which agrees with results plotted in Fig. 2.

The dependence upon the initial damage D_0 of the instability strain, and the corresponding damage D_{I} at the onset of instability normalized by the initial damage is shown in Fig. 3. The instability strain decreases from 0.081 to 0.0775 when the initial damage is increased from 0 to 0.05. The variations of the instability strain and the damage at the onset of instability with the normal anisotropy factor R, the strain rate in the x-direction, and material parameters m, n and ν are depicted in Figs. 4–7 and 8, respectively. It is evident that only the strain hardening exponent n, and the thermal softening exponent ν significantly affect the instability strain. Thus values of these parameters need to be determined more accurately than those of other parameters to ascertain a reliable value of the instability strain. Whereas the instability strain increases with an increase in n, it decreases with an increase in ν.

Experimental work of Fyfe and Rajendran [40] and finite-element simulations by Tuğcu [41] have shown that the ductility of a material increases with an increase in the inertia effects. Batra [42] and Batra and Lear

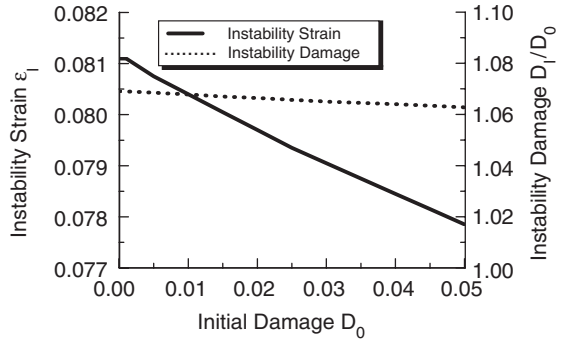

Fig. 3. Dependence upon the initial damage D_0 of the instability strain and the corresponding damage ratio D_I/D_0

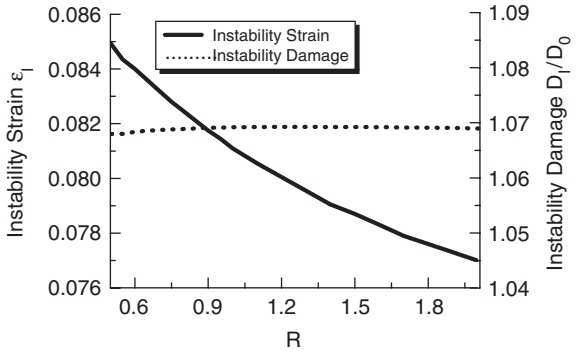

Fig. 4. Dependence upon the normal anisotropy factor R of the instability strain and the corresponding damage ratio D_I/D_0.

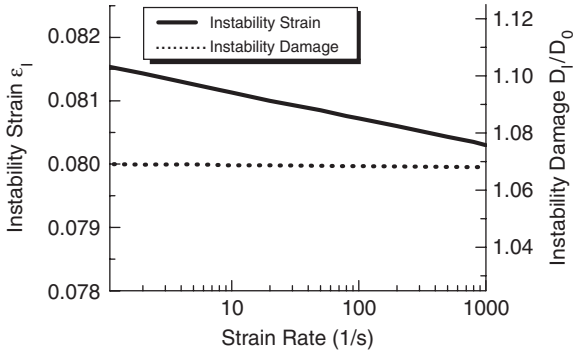

Fig. 5. Dependence upon the strain rate in the x-direction of the instability strain and the corresponding damage ratio D_I/D_0.

[37] concluded through numerical experiments that the strain at which an adiabatic shear band initiates increases with an increase in the applied nominal strain rate or equivalently with an increase in the inertia effects. For a microporous material Wu et al. [43] found that inertia effect is small in the early stages of void growth and it strongly depends upon the initial size of the void. However, under extremely high loading rates inertia effects first impede void growth but eventually promote void growth. Rajendran and Fyfe [44] analyzed the expansion of a ring under different strain rates and concluded that an increase in inertia effects enhanced the ductility of material of the ring.

Most studies on instability of sheets employ the Marciniak–Kuczynski criterion to delineate sheet necking. Ghosh [45], Brunet and Morestin [46] and Campos et al. [47] have studied the sheet metal forming of strain- and strain-rate hardening materials obeying a power-law-type relation, and found that the strain hardening

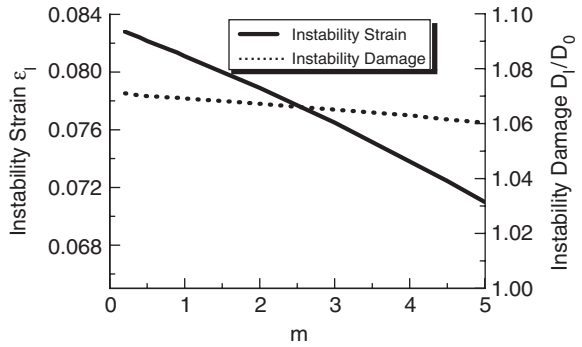

Fig. 6. Dependence upon the strain-rate hardening exponent, m, of the instability strain and the corresponding damage ratio D_I/D_0.

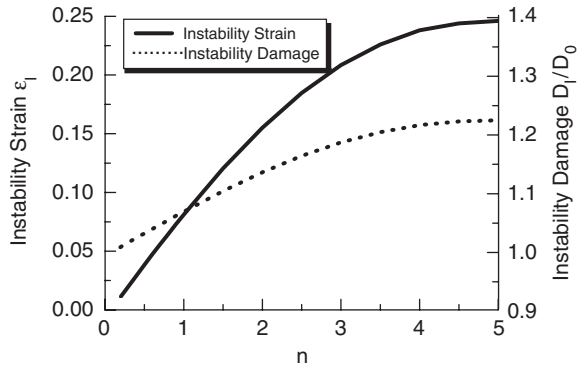

Fig. 7. Dependence upon the strain hardening exponent, n, of the instability strain and the corresponding damage ratio D_I/D_0.

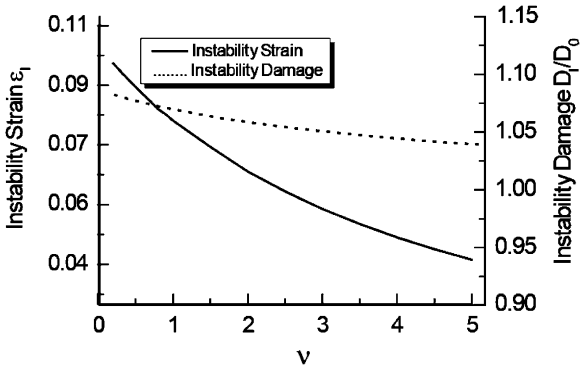

Fig. 8. Dependence upon the thermal softening exponent, ν, of the instability strain and the corresponding damage ratio D_I/D_0.

exponent strongly influences sheet necking. The instability strain increases with an increase in the value of the strain hardening exponent.

It is rather difficult to compare the computed instability strain with that either found experimentally or by other theories. Goto et al. [48] have accounted for the effect of anisotropy in HY100 steel and have developed a plasticity theory based on slip systems but ignoring the effect of damage and did not compute the instability strain.

The instability strain given by Eq. (43) usually corresponds to the peak in the effective stress–the effective strain curve. Numerical experiments analyzing 1D, 2D and 3D [27,36,49] transient problems for thermoelastoviscoplastic materials have shown that the effective plastic strain at the initiation of an adiabatic shear band is much higher than that at which the effective stress peaks; for a given material the difference

between the two is a function of the effective plastic strain rate, the thermal softening characteristics, and the rate of damage evolution. The effective plastic strain at failure is generally a little higher than that at the initiation of an adiabatic shear band. For 11 materials Batra and Lear [37] have listed in Table 3 of their paper the instability strain and the strain at the initiation of an adiabatic shear band; the ratio between the strain at the initiation of an adiabatic shear band and that at the onset of an instability varies from a low of 2.25 for copper to a high of 93 for a tungsten heavy alloy. We note that the strain at the initiation of an adiabatic shear band depends upon the size, type, and number of defects in the body.

4. Possible extension to spallation

Another important application of a damage model is to study spallation [1]. The influence of plastic anisotropy on spallation has not been investigated. However, the effect of material anisotropy should not be underestimated. As pointed out by Grady, the mode of deformation depends on the degree of anisotropy in the strain field [50]. It is common to compare the simulated rear-surface velocity with that observed experimentally, and then estimate the spallation strength, and the spallation time [22,23,51]. The simulation usually requires sophisticated computer codes.

We note that spall evolution in 1020 steel under multiaxial loading has been studied by Randers-Pherson and Rajendran [52]. Campagne et al. [53] have simulated spallation in HY-100 conical targets but it is hard to compare the two sets of results.

Here we use Grady's idea, and focus on analyzing the influence of anisotropy of a plastic material on spallation. Assume that the energy-limited spall gives the ductile spall strength $P_s = \sqrt{2\rho c_0^2 W_c}$, the spall or the fracture time, $t_s = \sqrt{2W_c \big/ \rho c_0^2 \dot{\varepsilon}^2}$, and the fragment size $s = \sqrt{8W_c \big/ \rho \dot{\varepsilon}^2}$. Note that all three are increasing functions of the critical dissipated work W_c. If the material mass density ρ, wave speed c_0, and the strain rate $\dot{\varepsilon}$ are constants, then values of P_s, t_s and s depend only on the dissipated plastic work. Grady estimated $W_c = \hat{Y}\varepsilon_c$, where $\hat{Y}$ is material's strength, ε_c a critical strain at which the void growth becomes unstable, namely, voids begin to coalesce. Grady [50] used $\varepsilon_c = 0.15$, or the critical porosity of 0.162 for all materials he studied. Seaman et al. [54] suggest that copper specimens fail when the porosity equals 0.3. However, for an anisotropic material the critical damage criterion should be direction dependent.

We first check whether or not Considere's criterion can be used to calculate ε_c. We assume that Eq. (56) also gives the critical strain at the onset of spallation. We recall that Considere's condition was initially proposed for uniaxial stress loading, while here the material at the sheet center is in a state of hydrostatic tension. For high mean tensile stresses, the damage Eq. (34) is not applicable. From simple geometric and mass conservation considerations we can deduce that

$$D = 1 - e^{-\varepsilon} \tag{57}$$

which is equivalent to $dD/d\varepsilon = e^{-\varepsilon} = (1 - D)$ or $dD/dt = e^{-\varepsilon}\dot{\varepsilon} = (1 - D)\dot{\varepsilon}$. Eq. (57) is the same as that used by Batra and Jaber [38] when the nucleation and coalescence of voids is neglected.

We note that in Eq. (56) $\frac{1}{\theta_m - \theta}\frac{d\theta}{d\varepsilon} \Big/ \frac{q}{1-D}\frac{dD}{d\varepsilon} = \frac{1}{7} - \frac{1}{5}$ for material parameters given in Table 1. The effect of damage in Eq. (57) is larger than that in Eq. (34). Thus neglecting the term related to thermal softening does not change the general trend of the instability strain but makes the physical meaning more clear. From Eqs. (51), (56) and (57), we get the following expression for the instability strain:

$$\varepsilon_c = \frac{Z(n - \varepsilon_y) - \varepsilon_y}{Z + 1}, \tag{58}$$

where $Z = \sqrt{2/3((R+2)/(R+1))}$ since for uniaxial loading $\alpha = 0$. However, ε_c is negative for $Z < 1.5$ meaning that the system is always unstable for the range of parameters used. The consideration of the thermal softening effect will decrease the instability strain. Thus Considere's criterion can not be used to determine ε_c.

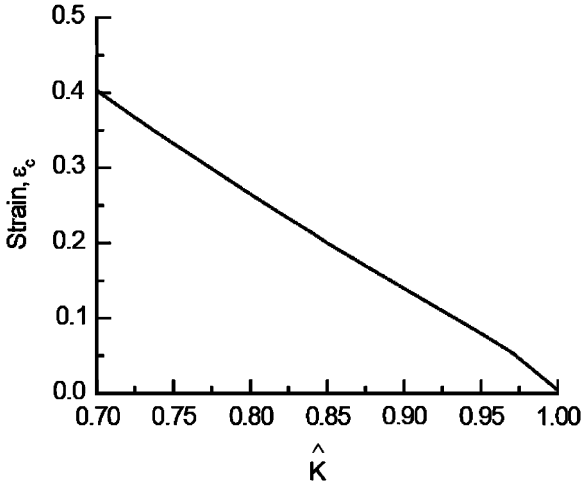

Fig. 9. Dependence of the critical strain, ε_c, upon the stress decrease, $\hat{K} = \sigma/\sigma_m$.

Batra and Kim [55] used the stress drop $\sigma/\sigma_{max} = \hat{K}$ as a criterion for the initiation of localized deformation. We note that spallation may also be viewed as a deformation and damage localization event. Here σ_{max} and ε_{max} are the maximum stress and the maximum strain, respectively, determined by setting $d\sigma/d\varepsilon = 0$. Using the constitutive relation (51), ignoring the temperature and the strain rate effects, and using Eq. (57), we get

$$\varepsilon_{max} = n - \varepsilon_y \tag{59}$$

and the critical strain ε_c can be determined from

$$\left(\varepsilon_c + \varepsilon_y\right)^n e^{-\varepsilon_c} = \hat{K} n^n e^{-(n-\varepsilon_y)}. \tag{60}$$

As depicted in Fig. 9 ε_c is a decreasing function of $\hat{K}$. For the criterion used by Grady [50], $\varepsilon_c = 0.15$, and we get $\hat{K} = 0.89$. In Batra and Kim [55], values of $\hat{K}$ equal to 0.8, 0.90, and 0.95 have been used as the localization criterion. The plastic work dissipated is given by $W_c = \int_0^{\varepsilon_c} \sigma \, d\varepsilon$. Once W_c is known, the spall strength, the time to fracture, and the fragment size can be calculated by using Grady's [50] relations.

5. Remarks

The present work illuminates which material parameters noticeably affect the instability strain during plane stress deformations of a thin sheet. The assumption that initially spherical voids grow as spheres during plastic deformations of an anisotropic material has simplified the analysis. However, in reality spheres become ellipsoids even when the state of stress is hydrostatic. For example, recent experiments [56] show that the shape of a void not only depends on the initial metallurgical structure of materials but also on the material anisotropy and loading conditions. The ratio of principal axes of elongated voids is found to be as large as 50. Thus, both anisotropic damage evolution and material anisotropy should be considered simultaneously in future works.

6. Conclusions

We have derived an expression for damage growth in an anisotropic material, and used it to analyze the stability of a thin sheet under a plane state of stress. It is assumed that the sheet becomes unstable when axial loads in the two principal directions at a point simultaneously reach their peak values. For the material of the sheet exhibiting strain and strain rate hardening, and thermal and damage softening, it is found that the strain hardening and thermal softening exponents strongly influence the axial strain when the sheet becomes unstable. The spallation of anisotropic materials is briefly discussed.

Acknowledgements

This work was partially supported by the Office of Naval Research Grants N00014-98-1-0300 and N00014-06-1-0567 to Virginia Polytechnic Institute and State University (VPI&SU) with Dr. Y.D.S. Rajapakse as the program manager. Views expressed herein are those of the authors and neither of the funding agency nor of VPI&SU.

References

[1] Curran DR, Seaman L, Shockey DA. Dynamic failure of solids. Phys Rep 1987;147:253–388.
[2] Voyiadjis GZ, Palazotto AN, Gao XL. Modeling of metallic materials at high strain rates with continuum damage mechanics. Appl Mech Rev 2002;55:481–93.
[3] Rice JR, Tracey DM. On the ductile enlargement of voids in triaxial stress fields. J Mech Phys Solids 1969;17:210–7.
[4] Gurson AL. Continuum theory of ductile rupture by void nucleation and growth: Part I—yield criteria and flow rules for porous ductile media. J Eng Mater Technol 1977;99:2–15.
[5] Ke FJ, Bai YL, Xia MF. Evolution of ideal micro-crack system. Sci China (Ser A) 1990;33:1447–59.
[6] Bai YL, Ke FJ, Xia MF. Formulation of statistical evolution of microcracks in solids. Acta Mech Sinica 1991;7:59–66.
[7] Bai YL, Ling Z, Luo LM, Ke FJ. Initial development of microdamage under impact loading. J Appl Mech 1992;59:622–7.
[8] Bai YL, Bai J, Li HL, Ke FJ, Xia MF. Damage evolution, localization and failure of solids subjected to impact loading. Int J Impact Eng 2000;24:685–701.
[9] Bai YL, Xia MF, Ke FJ, Li HL. Statistical microdamage mechanics and damage field evolution. Theor Appl Fract Mech 2001;37:1–10.
[10] Wei ZG, Batra RC. Dependence of instability strain upon damage in thermoviscoplastic materials. Arch Mech 2002;54:691–707.
[11] Liao KC, Pan J, Tang SC. Approximate yield criteria for anisotropic porous ductile sheet metals. Mech Mater 1997;26:213–26.
[12] Chien WY, Pan J, Tang SC. Modified anisotropic Gurson yield criterion for porous ductile sheet metals. J Eng Mater Technol 2001;123:409–16.
[13] Hill R. A theory of the yielding and plastic flow of anisotropic metals. Proc Roy Soc London Ser A 1948;193:281–97.
[14] Hill R. The mathematical theory of plasticity. Oxford: Oxford University Press; 1950.
[15] Carroll MM, Holt AC. Static and dynamic pore-collapse relations for ductile porous materials. J Appl Phys 1972;43:1626–36.
[16] Johnson JN. Dynamic fracture and spallation in ductile solids. J Appl Phys 1981;52:2812–5.
[17] Huang Y, Hutchinson JW, Tvergaard V. Cavitation instabilities in elastic–plastic solids. J Mech Phys Solids 1991;39:223–41.
[18] Huang Y. Accurate dilatation rates for spherical voids in triaxial stress fields. J Appl Mech 1991;58:1084–6.
[19] Molinari A, Wright TW. A physical model for nucleation and early growth of voids in ductile materials under dynamic loading. J Mech Phys Solids 2005;53:1476–504.
[20] Hanim S, Ahzi S. A unified approach for pressure and temperature effects in dynamic failure criteria. Int J Plasticity 2001;17:1215–44.
[21] Zhang CS, Zou S, Zhang BP. Damage evolution of ductile material under impact loading. Mech Res Commun 2006;33:26–34.
[22] Seaman L, Curran DR, Shockey DA. Computational models for ductile and brittle fracture. J Appl Phys 1976;47:4814–26.
[23] Feng JB, Jing FQ, Zhang GR. Dynamic ductile fragmentation and the damage function model. J Appl Phys 1997;81:2575–8.
[24] Li HL, Huang ZP. A statistical model of microvoids' evolution in rate sensitive ductile materials: solution for high stress triaxiality cases. Int J Damage Mech 1999;8:41–60.
[25] Considère A. L'emploi du fer et L'acier Dans Les Constructions. Ann Ponts Chaussées 1885;9:574–775.
[26] Swift W. Plastic instability under plane stress. J Mech Phys Solids 1952;1:1–18.
[27] Mellor PB. Plastic instability in tension. The Engineer 1960;209:517–21.
[28] Moore GG, Wallace JF. The effect of anisotropy on instability in sheet-metal forming. J Inst Met 1964;93:33–8.
[29] Hill R. On discontinuous plastic states with special reference to localized necking in thin sheets. J Mech Phys Solids 1952;1:19–30.
[30] Hecker SS. Formability of aluminum alloy sheet. ASME J Eng Mater Technol 1975;97:66–73.
[31] Keeler S.P., Plastic instability and fracture in sheets stretched over rigid punches. ScD thesis, Massachusetts Institute of Technology, Cambridge, MA, 1961.
[32] Marciniak Z, Kuczynski K. Limit strains in the process of stretch-forming sheet metals. Int J Mech Sci 1967;9:609–20.
[33] McGinty RC, McDowell DL. Application of multiscale crystal plasticity models to forming limit diagrams. J Eng Mater Technol 2004;126:285–90.
[34] Batra RC. Steady state penetration of thermoviscoplastic targets. Comput Mech 1988;3:1–12.
[35] Litonski J. Plastic flow of a tube under adiabatic torsion. Bull Acad Pol Sci 1977;25:7–17.
[36] Batra RC, Kim CH. Effect of thermal conductivity on the initiation, growth and band width of adiabatic shear bands. Int J Eng Sci 1991;29:949–60.
[37] Batra RC, Lear MH. Adiabatic shear banding in plane strain tensile deformations of eleven thermoelastoviscoplastic materials with finite thermal wave speed. Int J Plasticity 2005;21:1521–45.
[38] Batra RC, Jaber NA. Failure mode transition speeds in an impact loaded prenotched plate with four thermoviscoplastic relations. Int J Fract 2001;110:47–71.
[39] Müschenborn W, Sonne H. Influence of the strain path on the forming limits of sheet metal. Arch Eisenhüttenwes 1975;46:597–602.

[40] Fyfe IM, Rajendran AM. Dynamic pre-strain and inertia effects on the fracture of metals. J Mech Phys Solids 1980;28:17–26.
[41] Tuğcu P. Inertial effects in ductile failure of cylindrical tubes under internal pressure. Int J Impact Eng 1996;18:539–63.
[42] Batra RC. Effect of nominal strain-rate on the initiation and growth of adiabatic shear bands in steels. J Appl Mech 1988;55:229–30.
[43] Wu XY, Ramesh KT, Wright TW. The dynamic growth of a single void in a viscoplastic material under transient hydrostatic loading. J Mech Phys Solids 2003;51:1–26.
[44] Rajendran AM, Fyfe IM. Inertia effects on the ductile failure of thin rings. J Appl Mech 1982;49:31–6.
[45] Ghosh AK. The influence of strain hardening and strain-rate sensitivity on sheet metal forming. J Eng Mater Technol 1977;99:264–74.
[46] Brunet M, Morestin F. Experimental and analytical necking studies of anisotropic sheet metals. J Mater Process Technol 2001;112:214–26.
[47] Campos HB, Butuc MC, Grácio JJ, Rocha JE, Duarte JMF. Theoretical and experimental determination of the forming limit diagram for the AISI 304 stainless steel. J Mater Process Technol 2000;179:56–60.
[48] Goto DM, Bingert JF, Reed WR, Garrett RK. Anisotropy-corrected MTS constitutive strength modeling in HY-100 steel. Scr Mater 2000;42:1125–31.
[49] Batra RC, Wang, Zhicun. Failure mode transition speed in three-dimensional transient deformations of a microporous heat-conducting thermoelastoviscoplastic prenotched plate. J Therm Stresses 2005;28:533–62.
[50] Grady DE. The spall strength of condensed matter. J Mech Phys Solids 1988;36:353–84.
[51] Rajendran AM, Dietenberger MA, Grove DJ. A void growth-based failure model to describe spallation. J Appl Phys 1989;65:1521–7.
[52] Randers-Phreson G, Rajendran, AM. Evolution of spall under multiaxial loading. In: Batra RC, editor. Constitutive laws theory experiments and numerical experimentation, 1995. p. 52–61.
[53] Campagne L, Daridon L, Ahzi S. A physically based model for dynamic failure in ductile metals. Mech Mater 2005;37:869–86.
[54] Seaman L, Barbee JR, Curran DR. Dynamic fracture criteria of homogeneous materials, AFWAL-TR-71-156, Stanford Research Institute.
[55] Batra RC, Kim CH. Analysis of shear banding in twelve materials. Int J Plasticity 1992;8:425–52.
[56] Benzerga AA, Besson J, Pineau A. Anisotropic ductile fracture—Part I: experiments. Acta Mater 2004;52:4623–38.